Phytotaxa 372 (1): 051–066
http://www.mapress.com/j/pt/

Article

ISSN 1179-3155 (print edition)
PHYTOTAXA
ISSN 1179-3163 (online edition)

https://doi.org/10.11646/phytotaxa.372.1.4

The polyphasic approach revealed new species of *Chloroidium* (Trebouxiophyceae, Chlorophyta)

TATYANA DARIENKO[1,2], ALENA LUKEŠOVÁ[3] & THOMAS PRÖSCHOLD[4]
[1] *University of Göttingen, Experimental Phycology and Culture Collection of Algae, D-37073 Göttingen, Germany*
[2] *M.G. Kholodny Institute of Botany, National Academy Science of Ukraine, Kyiv 01601, Ukraine*
[3] *Biology Centre, Czech Academy of Sciences, Institute of Soil Biology, 37005 České Budějovice, Czech Republic*
[4] *University of Innsbruck, Research Institute for Limnology, A-5310 Mondsee, Austria*
Correspondence: Thomas Pröschold, E-mail: Thomas.Proeschold@uibk.ac.at

Abstract

Chlorella-like coccoid green algae are widely distributed in many types of habitats such as freshwater, terrestrial and marine. One group of terrestrial microalgae belonging to the Trebouxiophyceae forms the monophyletic lineage of the *Watanabea* clade. This clade exclusively comprises of ellipsoid and spherical coccoid green algae, which traditionally have been assigned as different species of *Chlorella*. Within this clade, seven out of ten genera are described mainly based on phylogenetic analyses of SSU and *rbc*L sequences. Most of the genera are represented by only one or two species that are rarely found in natural samples. In contrast, the genus *Chloroidium* is widely distributed across different habitats. We investigated 34 new isolates, which were originally assigned as *Chloroidium* or *Chlorella*, using an integrative approach. The phylogenetic analyses of SSU and ITS rDNA sequences revealed nine lineages, eight of which were highly supported in all of our bootstrap and Bayesian analyses. The ITS-2/CBC approach clearly demonstrated that these nine lineages represent individual species. The haplotype network analyses revealed that three out of them were widely distributed and showed no preference for any habitat.

The comprehensive study of SSU and *rbc*L datasets also revealed that no clear synapomorphy could be found to support the assigned genus *Parachloroidium*. As a result of our findings, we proposed that both species belonging to *Parachloroidium* be transferred to *Chloroidium*. In addition, we re-established two species originally described by Chodat as new members of *Chloroidium* (*C. lichenum*, *C. viscosum*). Two of the nine lineages (*C. antarcticum*, *C. arboriculum*) were newly described in this study.

Keywords: integrative taxonomy, *Chloroidium*, intraspecific variation, species concept, DNA barcoding

Introduction

Small *Chlorella*-like (smaller than 10 µm and reproducing by autospores) coccoid green algae (including photobionts of lichens) are widely distributed in different terrestrial and aquatic habitats. Phylogenetic studies of SSU rDNA sequences have shown that this group of organisms is polyphyletic and belongs to two classes Chlorophyceae and Trebouxiophyceae (Huss *et al.*, 1999, Krienitz & Bock, 2012 and references therein). Ellipsoidal chlorelloid algae are members of the class Trebouxiophyceae and belong to the *Watanabea*-clade. The historical background, morphology and taxonomy of these organisms were clarified by Darienko *et al.* (2010). They emended the genus *Chloroidium* Nadson and transferred all ellipsoid taxa previously assigned as *Chlorella saccharophilum*, *C. ellipsoideum*, and *C. angustoellipsoideum* to this genus. Along with *Chloroidium* the following *Chlorella*-like taxa belong to the *Watanabea* clade: *Watanabea* (Hanagata *et al.*, 1998), *Viridiella* (Albertano *et al.*, 1991), *Heveochlorella* (Zhang *et al.*, 2008, Ma *et al.*, 2013), *Kalinella* (Neustupa *et al.*, 2009, 2013a), *Parachloroidum* (Neustupa *et al.*, 2013b), *Desertella* (Fučíková *et al.*, 2014, Song *et al.*, 2016), *Mysteriochloris* (Song *et al.*, 2016), *Polulichloris* (Song *et al.*, 2015), and *Phyllosiphon* (Aboal & Werner, 2011, Procházková *et al.*, 2015, 2016, 2018, Song *et al.*, 2016). Morphologically, the genera of the *Watanabea* clade could be divided into two morphological groups: (i) species with ellipsoidal cells (*Chloroidium*, *Watanabea*, *Viridiella*, *Polulichloris*, and *Desertella*) and (ii) those with spherical cells (*Heterochlorella*, *Kalinella, Mysteriochloris, Phyllosiphon,* and *Parachloroidium*). Morphological identification of these genera is very difficult for

Accepted by Karolina Fucíková: 14 Sept. 2018; published: 10 Oct. 2018

the most part. For example, the recently described genera *Polulichloris* and *Desertella* share the same morphological features as *Chloroidium ellipsoideum*, but represent separate, distinct lineages in SSU and *rbc*L phylogenies. Spherical members of this clade cannot be clearly distinguished by morphology alone. All species belonging to the *Watanabea* clade can only be clearly identified by the application of molecular data to determine the exact phylogenetic affiliation at the species or even at the generic level.

In our study, we investigated more than 50 algal strains assigned as *Chloroidum saccharophilum*, *C. ellipsoideum*, *C. angustoellipsoideum* or *Chloroidium* sp. using a polyphasic approach and compared them with authentic strains of two described species of *Parachloroidium*.

The aim of our study was to prove the possible hidden diversity in this group of organisms and to find the correlation among the molecular phylogeny, morphology and distribution of the investigated organisms. To compare these strains, we studied the morphology and phenotypic plasticity, analyzed the SSU and ITS rDNA using the same methods as described by Darienko *et al.* (2016), and compared the DNA and amino acid sequences of the plastid-coding *rbc*L gene.

Material and Methods

Strain origin, culture conditions and light microscopy

The investigated strains originated from the Culture Collection of Algae (SAG) at the University of Göttingen (Germany), the Culture Collection of Algae and Protozoa (CCAP, Scotland), working collection of soil algae and cyanobacteria of Alena Lukešová (ISB), which is now a part of Biology Centre Collection of Organisms (BCCO) at Biology Centre of the Czech Academy of Sciences (Czech Republic), and the personal collection Tatyana Darienko. Details about origin and habitat are summarized in Table S1 (Supplemental Material). All strains were cultivated at 20°C, with 50 µmol photons/m^2s^1 provided by daylight fluorescent tubes, Osram L36W/954 Lumilux de lux daylight, Munich, Germany), and light:dark cycle of 14:10 hrs. We used modified Bold's Basal Medium (3N-BBM+V; medium 26a in Schlösser, 1997) as culture medium.

For species identification, two-week-old cultures were selected using the identification keys of Fott & Nováková (1969) and Andreyva (1975). The morphology of the strains was compared with the original species descriptions. For the light microscopic investigations, an Olympus BX-60 microscope was used (Olympus, Tokyo, Japan) and the micrographs were taken with a Prog Res C14 plus camera using the Prog Res Capture Pro imaging system (version 2.9.0.1), both from Jenoptik, Jena, Germany).

DNA extraction, PCR, and sequencing

DNA extraction, PCR, and PCR purification and sequencing were conducted using the detailed protocol described in Darienko *et al.* (2016). The genomic DNA of the strains was extracted using the DNeasy Plant Mini Kit (Qiagen, Hilden, Germany) and following the instructions provided by the manufacturer. The SSU and ITS rDNA were amplified in PCR reactions using the Taq PCR MasterMix Kit (Qiagen, Hilden, Germany) with the primers EAF3 and ITS055R (Marin *et al.,* 2003). The *rbc*L gene was amplified using the primers (PrasF and EllaR; Neustupa *et al.*, 2013a) and methods described by Nozaki *et al.* (1995). All PCR products were purified and sequenced as described by Darienko *et al.* (2016). The sequences are available in the EMBL, GenBank and DDBJ sequence databases under the accession numbers given in Table S2 and Fig. 2.

Phylogenetic analyses

The SSU rDNA sequences of all strains were aligned according to their secondary structures. The ITS-1 and ITS-2 sequences of all strains were folded according to the protocol described in detail in Darienko *et al.* (2016). The alignments were separated into the following three datasets: (i) concatenated dataset of 58 SSU and ITS rDNA sequences of *Chloroidium* and *Parachloroidium* (2643 bp), and (ii) a dataset of 23 SSU rDNA (1790 bp) and (iii) a dataset of 23 *rbc*L (804 bp) sequences of representatives of all the genera belonging to the *Watanabea* clade of the Trebouxiophyceae. For analyses of the *rbc*L sequences, the third codon positions were saturated (tested using the program DAMBE; Xia, 2018) and therefore excluded from the dataset. In addition, the *rbc*L dataset of all codon positions (1206 bp) was used for codon base analysis and implemented in PHASE (YNH98 model; Yang *et al.*, 1998). The alignments are available in TreeBase under the number S23245. For all data sets the best evolutionary models were calculated with the program Modeltest 3.7 (Posada, 2008) using the Akaike Information Criterion (Akaike, 1974). The settings of the best models

are given in the figure legends. The following methods were used for the phylogenetic analyses: distance, maximum parsimony, maximum likelihood, and Bayesian inference. Programs used included PAUP version 4.0b10 (Swofford, 2002), RAxML version 7.0.3 (Stamatakis, 2006), MrBayes version 3.2.3 (Ronquist *et al.*, 2012), and PHASE package 2.0 (Jow *et al.*, 2002, Higgs *et al.*, 2003, Hudelot *et al.*, 2003, Gibson *et al.*, 2005, Telford *et al.*, 2005).

ITS-2 secondary structures and ITS-2/CBC approach

The secondary structures of ITS-2 sequences were folded using the computer programs mfold (Zuker, 2003), which used the thermodynamic model (minimal energy), and CONTRAfold (Do *et al.*, 2006), a program that used a stochastic approach for the RNA folding. The following three constraints were set for the folding: (1) the last 25 bases of the 5.8S rRNA and the first 25 of the LSU rRNA must bind and form the 5.8S/LSU stem, (2) the pyrimidine/pyrimidine mismatch (the first RNA processing site) after the 5–7th base pair in Helix II must be present in the structure, and (3) the second RNA processing site, the GGU motif characteristic for green algae, must be at the 5' site in Helix III (for details about the processing sites and constraints; see Coleman, 2003, Cote *et al.*, 2002).

The secondary structure models of ITS-2 derived from these folding results were then used for species delimitation within *Chloroidium*. For the ITS-2/CBC approach, the conserved region of ITS-2 was extracted following the procedure that was introduced for *Coccomyxa* by Darienko *et al.* (2015): it includes (1) 16 base pairs of the 5.8S/LSU stem, (2) five base pairs of Helix I, (3) eleven base pairs of Helix II including the pyrimidine-pyrimidine mismatch, and (4) all base pairs of Helix III. The resulting data set was then manually aligned. These alignments have been translated into base pair alignment by using a number code for each base pair (**1** = A-U; **2** = U-A; **3** = G-C; **4** = C-G; **5** = G•U; **6** = U•G; **7** = mismatch; **8** = deletion/insertion or single bases). The barcodes for each species were compared to detect for compensatory base changes (CBCs), hemi-CBCs (HCBCs), insertions/deletions, and single or unpaired bases.

Distribution and haplotype network analyses

For these analyses, the SSU and ITS rDNA dataset of the 58 investigated strains were subdivided into three groups representing SSU, ITS-1 and ITS-2. The haplotypes of each region were detected among these groups. The present haplotypes are summarized in Table S2. The metadata (geographical origin and habitat) of each strain belonging the different haplotypes are also given in this table. To establish an overview about the distribution of *Chloroidium*, the ITS-2 haplotypes was used for the BLAST N search (100% coverage, >97% identity; Altschul *et al.*, 1990). To construct the haplotype networks, we used the TCS network tool (Clement *et al.*, 2000, 2002) implemented in PopART (Leigh & Bryant, 2015) for *C. saccharophilum*, *C. ellipsoideum* and *C. lichenum*, when data about multiple strains were available.

Results

Molecular phylogeny of *Chloroidium* and *Parachloroidium*

All investigated strains belonged to *Chloroidium* and *Parachloroidium* in our phylogenetic analyses (Fig. 1; *Parachloroidium* are marked with an asterisk). They formed eight highly supported lineages in all of our bootstrap and Bayesian analyses, and three out of them were novel among *Chloroidium*/*Parachloroidium*. Most of the strains were almost identical to the authentic strains of *Chloroidium saccharophilum*, *C. ellipsoideum* and *C. angustoellipsoideum*. *C. angustoellipsoideum* represented a later synonym of *C. lichenum* (Chodat) comb. nov. (see below in Taxonomic consequences and revisions). New lineages included the strains SAG 56.87 and MG-2, ISBAL-1013, and MG-1 and MG-3, which represented their own species described below as *C. viscosum*, *C. antarcticum*, and *C. arboriculum*, respectively. *C. arboriculum* was a sister of the authentic strain of *Parachloroidium laureanum* (CAUP H8501) and represented an intermediate species between *Chloroidium* and *Parachloroidium* (see details below). The addition of new strains among *C. ellipsoideum*/*C. lichenum* resulted in an unresolved phylogeny within this subclade. Both species (*C. ellipsoideum* and *C. lichenum* subgroup B in Fig. 1 = *C. angustoellipsoideum*) as defined by Darienko *et al.* (2010) were still highly supported in all of our analyses, but the affiliation of new strains (*C. lichenum* subgroups A and C in Fig. 1) remained unresolved. The phylogenetic analyses showed that *C. saccharophilum*, *C. ellipsoideum* and *C. lichenum* had no preferences regarding geographical distribution and habitat as indicated in Fig. 1. It seemed that these species were widely distributed.

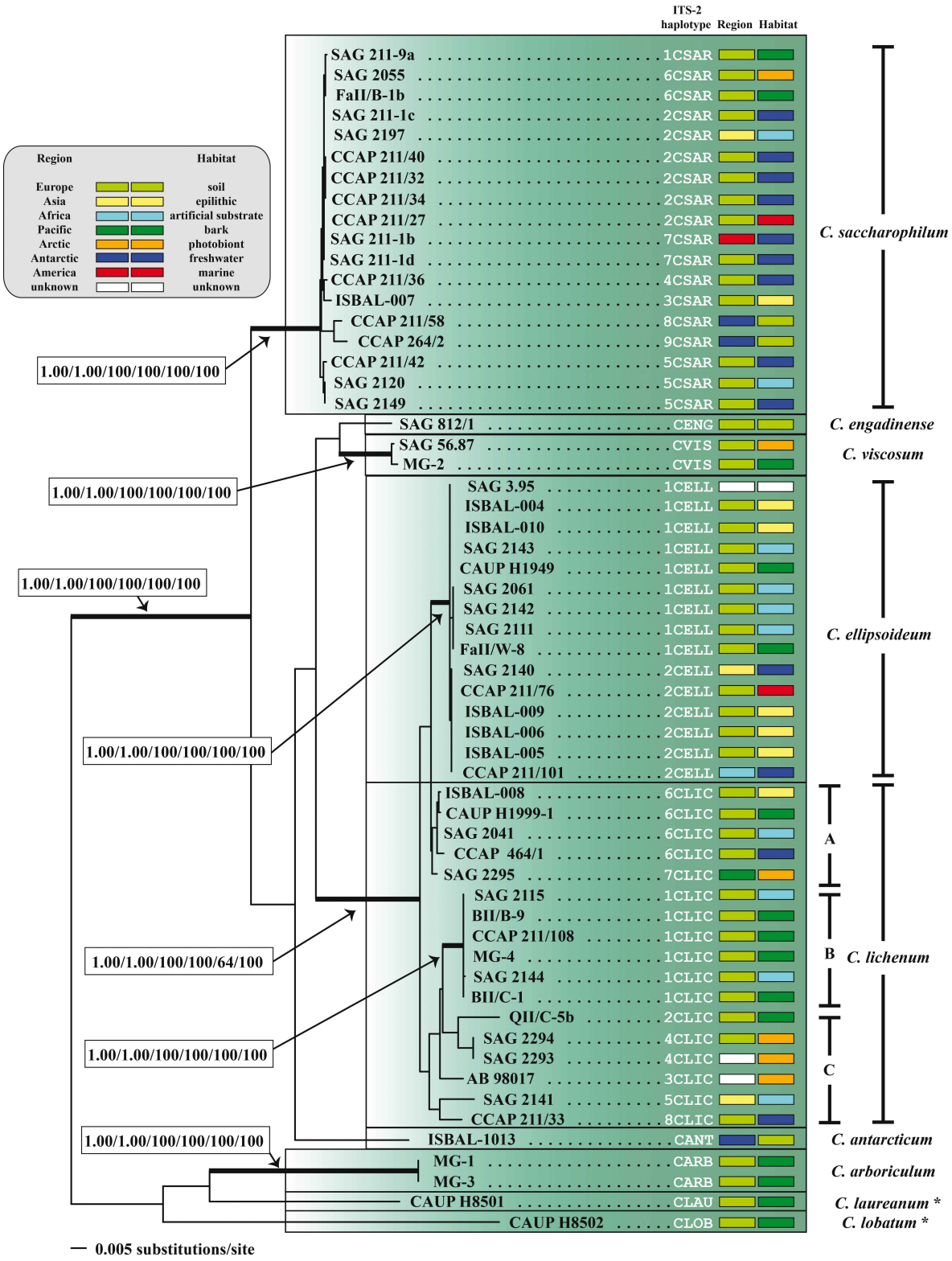

FIGURE 1. Molecular phylogeny of *Chloroidium* based on SSU and ITS rDNA sequence comparisons. The phylogenetic trees shown were inferred using the maximum likelihood method based on the data sets (2643 aligned positions of 58 taxa) using PAUP 4.0b10. For the analyses the best model was calculated by Modeltest 3.7. The setting of the best model was given as follows: GTR+I+G (base frequencies: A 0.2263, C 0.2597, G 0.2814, T 0.2326; rate matrix A-C 3.0220, A-G 3.2461, A-U 1.8828, C-G 1.0985, C-U 7.0041, G-U 1.0000) with the proportion of invariable sites (I = 0.7069) and gamma shape parameter (G = 0.6406). The branches in bold are highly supported in all analyses (Bayesian values > 0.95 calculated with PHASE and MrBayes; bootstrap values > 70% calculated with PAUP using maximum likelihood, neighbor-joining, maximum parsimony and RAxML using maximum likelihood). The taxa originally described as *Parachloroidium* were indicated by an asterisk. The ITS-2 haplotype designations as well as the geographical origins and habitats are given color-coded after the strain designations.

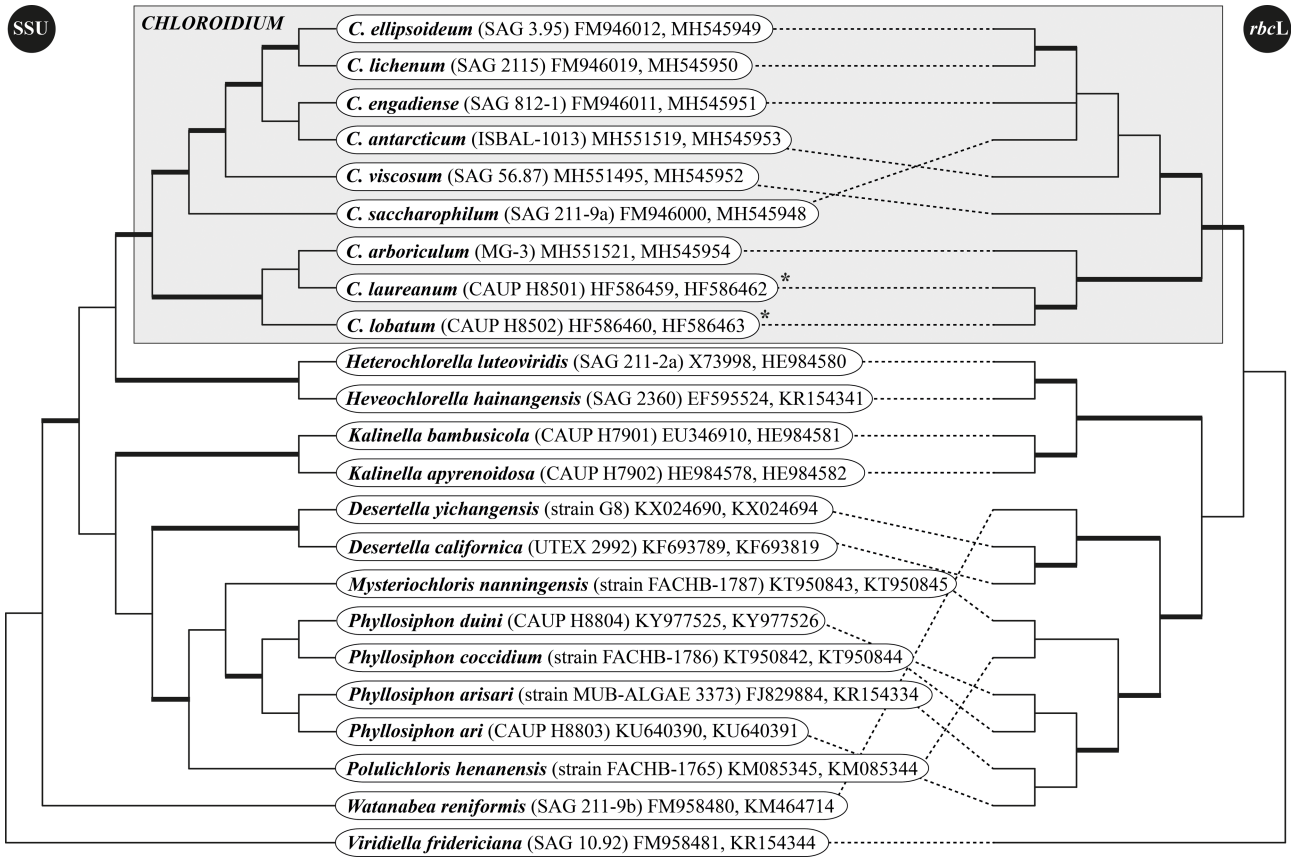

FIGURE 2. Molecular phylogeny of representatives belonging to the *Watanabea* clade based on *rbc*L and SSU rDNA sequence comparisons. The phylogenetic trees shown were inferred using the maximum likelihood method based on the data sets (23 taxa: 1790 aligned positions for SSU, 804 for *rbc*L) using PAUP 4.0b10. For the analyses the best model was calculated by Modeltest 3.7. The setting of the best model was given as follows: (**SSU**) TIM+I+G (base frequencies: A 0.2462, C 0.2339, G 0.2883, T 0.2316; rate matrix A-C 1.0000, A-G 2.2465, A-U 1.2966, C-G 1.2966, C-U 6.0538, G-U 1.0000) with the proportion of invariable sites (I = 0.5137) and gamma shape parameter (G = 0.6912); (***rbc*L**) GTR+I+G (base frequencies: A 0.2606, C 0.2247, G 0.2899, T 0.2248; rate matrix A-C 2.3970, A-G 1.2715, A-U 0.7452, C-G 0.5103, C-U 6.8373, G-U 1.0000) with the proportion of invariable sites (I = 0.6386) and gamma shape parameter (G = 0.2501). The branches in bold are highly supported in all analyses (Bayesian values > 0.95 calculated with PHASE and MrBayes; bootstrap values > 70% calculated with PAUP using maximum likelihood, neighbor-joining, maximum parsimony and RAxML using maximum likelihood). The Bayesian analysis in PHASE was calculated using the dataset of all three codon bases (1206 bp) and the codon model YNH98 (Yang *et al.* 1998).

Molecular phylogeny of the *Watanabea* clade

As demonstrated in Fig. 1, both genera *Chloroidium* and *Parachloroidium* were closely related, and the strains MG-1/MG-3 represented an intermediate species between both genera. This raised questions about the generic concept. Neustupa *et al.* (2013b) described *Parachloroidium* based on SSU and *rbc*L phylogeny and used a single synapomorphy in the *rbc*L gene (at position 286) as a diagnostic feature. To prove whether this synapomorphy remained and to obtain better insights about evolutionary rates, we analyzed the SSU and *rbc*L of all genera and species belonging to the *Watanabea* clade. For this comparison, we sequenced the *rbc*L of the representative *Chloroidium* lineages and incorporated these sequences into a representative dataset for members belonging to the *Watanabea* clade. For the analyses of the *rbc*L gene, the third codon positions were saturated, which were tested with the program DAMBE (see Figures S1; Supplemental Material) and therefore excluded from tree calculations. The phylogenetic analyses of both datasets (SSU and *rbc*L) demonstrated different tree topologies (Fig. 2 and Figs S1). However, the main lineages representing genera were resolved in both analyses, and only the relationship among the genera was different. The *Chloroidium*/*Parachlorodium* subclade remaining in SSU and *rbc*L phylogeny was highly supported in all of our analyses, but the support using the *rbc*L sequences was only high in the Bayesian analysis that used the codon model implemented in PHASE. The position of the strain MG-3 was different in both analyses. This strain was a sister of only CAUP H8501 in SSU rDNA phylogeny, but in *rbc*L phylogeny, it was a sister of both strains CAUP H8501 and CAUP

H8502. To analyze these discrepancies further, we compared the variability among these genes. The *rbc*L gene was analyzed at both levels (DNA and protein) to find synapomorphies. The variabilities among SSU, ITS, and *rbc*L (all three or first two codon bases) were very different. Within the *Watanabea* clade, the SSU rDNA sequences contained 483 variable positions (27.0%), in contrast to *rbc*L, which showed only 98 in the first two codon bases (12.2%). However, the variability among *Chloroidium*/*Parachloroidium* was very different (SSU: 61 variable positions = 3.4%; *rbc*L, first two codon bases: 49 = 6.1%). As demonstrated by Neustupa *et al.* (2013b), *Chloroidium*/*Parachloroidium* contained an additional amino acid (K = lysine) at position 78 in the protein alignment of *rbc*L. After analyzing the *rbc*L protein alignment, two more synapomorphies were discovered for (position 28: D = asparagine and position 80: F = phenylalanine) and against (position 71: A = alanine and position 235: R = arginine) the combination of the two genera to one genus. The unique base position at 286 (third codon base) found by Neustupa *et al.* (2013b) for the two *Parachloroidium* strains could be found at position 234 (G) in our alignment; however, this position was not unique because the strain MG-3 topologically closely related to both strains and shows the same base (A) like the other strains of *Chloroidium*.

Species concept among *Chloroidium*/*Parachloroidium* using the ITS-2/CBC approach

As demonstrated in Fig. 1, the investigated strains formed eight independent lineages within *Chloroidium*/*Parachloroidium*. The subclade *C. ellipsoideum*/*C. lichenum* was not clearly resolved in the SSU/ITS phylogeny. Therefore, we analyzed the ITS-2 secondary structures of all strains (Figs S2; Supplemental Material) to detect compensatory base changes (CBCs) for species delimitation. The ITS-2 haplotypes were marked in Fig. 1 and Table S2. Using the ITS-2/CBC approach described in detail in Darienko *et al.* (2016), the conserved region of each ITS-2 secondary structure was used as a barcode marker after its transformation into a unique numerical code (see Fig. 3). Twenty-five unique barcodes were observed among the 58 strains, which showed 19 CBCs and 23 HCBCs in their secondary structures (Fig. 3). The eight phylogenetic lineages representing species were supported by these CBCs/HCBCs. In addition, the strains belonging to the subclade *C. ellipsoideum*/*C. lichenum* could be subdivided into two lineages by a unique CBC at position 50 in the barcode alignment (Fig. 3). This subdivision was also supported by the phylogenetic analysis presented in Fig. 3.

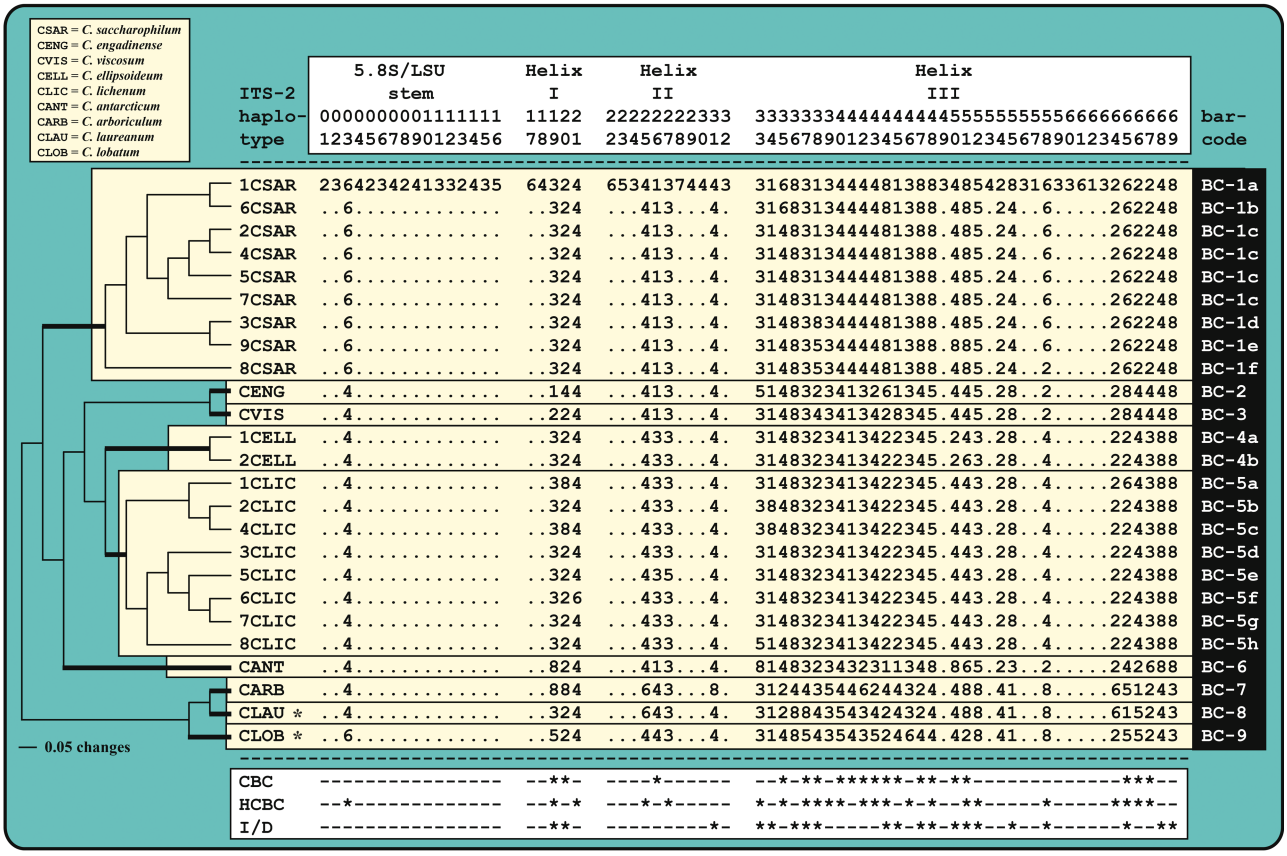

FIGURE 3. Comparison of the conserved region of ITS-2 among the species of *Chloroidium*. Extraction of this region and translation into a number code for its usage as barcode (extracted bases highlighted with an asterisk). Number code for each base pair: 1 = A-U; 2 = U-A; 3 = G-C; 4 = C-G; 5 = G•U; 6 = U•G; 7 = mismatch; 8 = deletion, single or unpaired bases.

Distribution of the haplotypes

To establish an overview of the distribution of all species, the ITS-2 sequences of all haplotypes were used in a BLAST N search. Using this approach (100% coverage, >97% identity), only entries for *C. saccharophilum* could be observed in GenBank. Another entry (FJ792803) originally assigned as *Symbiochloris reticulata*, a photobiont of the lichen *Lobaria pulmonaria*, instead represented the newly described species, *Chloroidium arboriculum*. The metadata (geographical origin and habitat) belonging to these entries were included with those of the exiting data for our investigated strains to create a dataset for the TCS analyses. The haplotype network analyses revealed a close relationship among the three species *C. saccharophilum* (Fig. 4) and *C. ellipsoideum*/*C. lichenum* (Fig. 5) using the program PopART. The 13 ITS-2 haplotypes of *C. saccharophilum* differed by only a few bases. Four out of them called 10CSAR-13CSAR (marked in gray boxes) represented entries only found in GenBank. Among the subclade *C. ellipsoideum*/*C. lichenum*, no new entries in GenBank were observed using the BLAST N search algorithm described above. The network analyses revealed that the haplotypes of the two species also differed by only a few bases that are mostly located between helix III and LSU (see secondary structures in Figs S2). As demonstrated in Fig. 4 and 5, all haplotypes of the species showed no preferences regarding geographical origin or habitat.

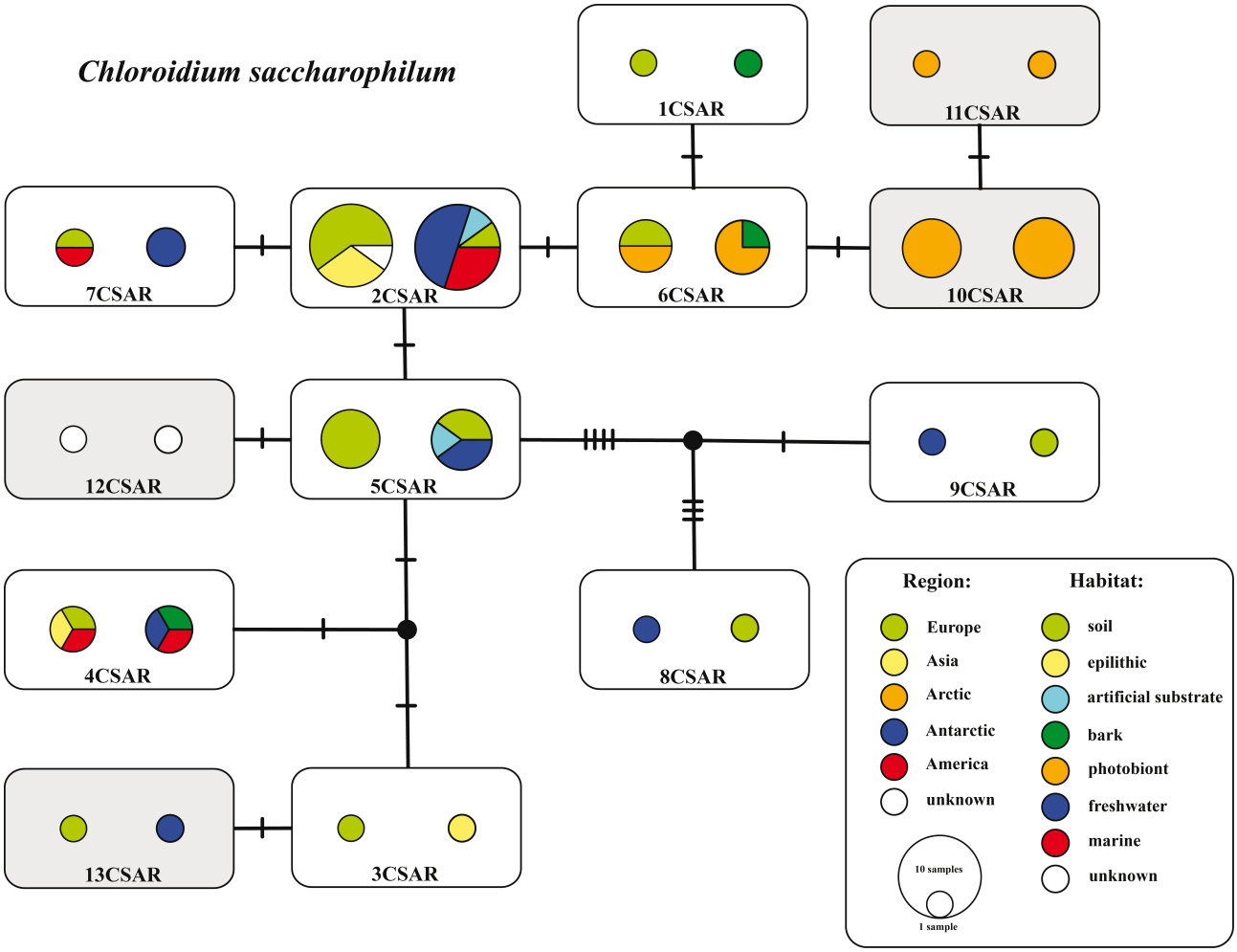

FIGURE 4. TCS haplotype network inferred from ITS-2 rDNA sequences of *Chloroidium saccharophilum*. This network was inferred using the algorithm described by Clement *et al.* (2002). Sequence nodes corresponding to samples collected from different geographical region and from different habitats.

Morphology and phenotypic plasticity of the *Chloroidium* species

The morphology and variability of known *Chloroidum* and *Parachloroidium* species were described in Darienko *et al.* (2010) and Neustupa *et al.* (2013b), respectively. Thirty of the newly investigated strains could be clearly assigned to the genus *Chloroidium* based on morphology. These strains showed an ellipsoid cell shape, the presence of unequally sized autospores, and parietal lobated chloroplasts with a pyrenoid. The strain ISBAL-1013 differed in its larger cell size and naked pyrenoid (Fig. 6A–G). In contrast to these strains, the four isolates (SAG 56.87, MG-1-3; see Fig. 6H–V) were characterized by a spherical cell shape and band-shaped chloroplasts, similar to the chloroplast

described for *Heterochlorella luteoviridis* (Chodat, 1913; therein assigned as *Chlorella luteoviridis*). These strains also showed unequally sized autospores during asexual reproduction and occasionally granulated cell walls. The present pyrenoid was barely visible without Lugol staining because of the lack of surrounding starch grains. These four strains represented morphologically intermediate taxa between the genera *Chloroidium* and *Parachloridium*. The detailed morphological descriptions of the new species are presented below in the diagnoses.

Discussion

Chloroidium versus *Parachloroidium*

All investigated strains belonged to *Chloroidium* and *Parachloroidium* as demonstrated in Fig. 1. The morphology of these strains was very similar and varied only in cell shape and size, chloroplast shape and the absence or presence of a pyrenoid (Darienko *et al.*, 2010, Neustupa *et al.*, 2013b, Fig. 6 in this study). The distinction of both genera is very difficult because of lack of any synapomorphy in morphology and in SSU/ITS and *rbc*L sequences. The typically spherical cell shape of *Parachloroidium* could also be find in new isolates of *Chloroidium*. Neustupa *et al.* (2013b) described a genetic synapomorphy (insertion) at position 286 in the *rbc*L gene for *Parachloroidium* and *Chloroidium*. This synapomorphy could also be observed in the new taxa of *Chloroidium*. Neustupa *et al.* (2013b) used the codon AAG for the separation of *Parachloroidium* from *Chloroidium* (which has AAA in the insertion), coding for the inserted amino acid *Lys*. The strains MG-1 and MG-3 topologically closely related to both species of *Parachloroidium,* showed the same amino acid coding (AAA) and therefore represented genetic intermediates between *Chloroidium* and *Parachloroidium*. Considering both strains as new species of *Parachloroidium*, the genetic variability among the strains of *Chloroidium* and *Parachloroidium* was very similar, but was very low compared to other genera and species of the *Watanabea* clade. For example, both species of *Kalinella* differed by 152 and 12 bases in the SSU rDNA and *rbc*L sequences, respectively. Summarizing, *Parachloroidium* with the inclusion of the strains MG-1 and MG-3 does not show any morphological or molecular characters for recognition as separated genus. Therefore, as a result of our findings (no morphological differences, only a few genetic synapomorphies, low genetic variability), we transfer *Parachloroidium* and both of its described species to the emended genus *Chloroidium* (see below in taxonomic consequences and revisions).

Species concept and distribution of *Chloroidium* species

As demonstrated in Figs 1–6, the investigated strains represented nine phylogenetic lineages among the genus *Chloroidium*. Morphologically, the cells of these strains showed ellipsoid and spherical cell shape and parietal or band-shaped chloroplasts with or without pyrenoids. This clearly demonstrated that the species were difficult to identify using solely morphology for species delimitation. Darienko *et al.* (2010) have shown that *C. angustoellipsoideum* (now *C. lichenum* see below) was highly phenotypically polymorphic and could only be separated from *C. ellipsoideum* by molecular phylogeny. The addition of new strains to *Chloroidium* not only changed the previous framework at the species level, but also questioned the structure at the generic level. Previously, only species and strains with an ellipsoid cell shape were assigned to *Chloroidium*, but with the addition of these new strains, spherical species and strains could also be included in this genus, which clearly questions the construction of *Parachloroidium* as a separate genus as discussed above. Our phylogenetic analyses clearly revealed that spherical and ellipsoid taxa were mixed; therefore, these taxa represented only one monophyletic lineage within the *Watanabea* clade. Because of the lack of diagnostic morphological features, we used the ITS-2/CBC approach introduced by Darienko *et al.* (2015) for species discrimination. As shown in Fig. 3, nine lineages representing species could be clearly distinguished by CBCs and HCBCs. Even *C. ellipsoideum* and *C. lichenum*, which were not resolved in the phylogenetic analyses presented in Fig. 1, were separated by unique CBC in the conserved region of ITS-2. The variability within the subclade *C. ellipsoideum*/*C. lichenum* was much higher than in the other species of *Chloroidium* as described above, which is probably the reason that both species were not clearly separated in our analyses. In this study, we followed the approach introduced by Coleman (2000) for biological species. If two specimen differ in at least one CBC in the conserved region of ITS-2, they cannot mate. Despite that *Chloroidium* species only reproduce asexually, this approach seemed appropriate for asexually reproducing taxa, as several studies have shown (Darienko *et al.*, 2015a, b, 2016, Demchenko *et al.*, 2012, Pröschold *et al.*, 2018).

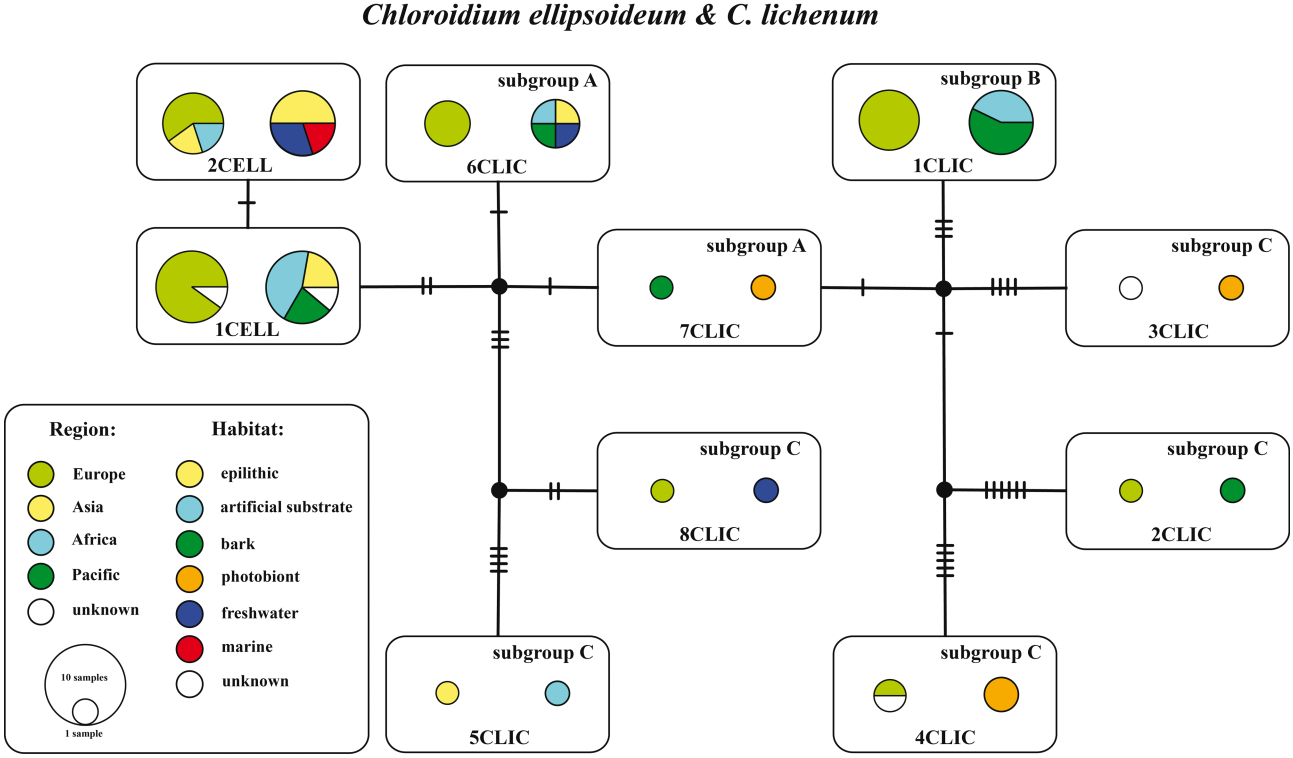

FIGURE 5. TCS haplotype network inferred from ITS-2 rDNA sequences of *Chloroidium ellipsoideum* and *C. lichenum*. This network was inferred using the algorithm described by Clement *et al.* (2002). Sequence nodes corresponding to samples collected from different geographical region and from different habitats.

The different *Chloroidium* species are widely distributed in different habitats around the world (Ettl & Gärtner, 1995, 2014; designated therein as *Chlorella saccharophila* and *C. ellipsoidea*). However, as demonstrated in Figs 4-5, only few records of *Chloroidium,* mainly of *C. saccharophilum*, were observed in environmental studies. Our network analyses confirmed this distribution pattern even though most available genetic data originated from European habitats. Data from other continents were underrepresented in GenBank. The lack of genetic data in GenBank could be caused by the presence of introns in SSU rDNA sequence. Forty-one out of 58 investigated strains had at least one intron, and some even contained two or three (see Table S2). The presence of introns could make it difficult to acquire PCR products for NGS approaches (V4 or V9 region of SSU). *Chloroidium* species were observed in different terrestrial habitats using cloning approaches (Hallmann *et al.*, 2016).

Taxonomic consequences and revisions

Many microalgae have been described in different types of terrestrial habitats, such as soil, rocks, and tree bark, and as photobionts of lichens (see Ettl & Gärtner, 1995, 2014). Within the genus *Chlorella* (in the traditional sense), a number of species were discovered by Chodat (1913) on the surface of several *Cladonia* lichens. Chodat often used media with gelatin and different sugars for the investigations, which makes it difficult to compare the morphology of his samples with those of current standard media. *Chlorella lichina* Chodat, *C. lacustris* Chodat, *C. rugosa* Chodat, *C. cladoniae* Chodat, and *C. viscosa* Chodat are definitely members of the *Watanabea* clade and share the same morphological features and ecology with species of *Chloroidium* and *Parachloroidium*. This is recognizable by the presence of unequally sized autospores, the presence of pyrenoids, and the structure of the chloroplast. The taxonomic status of these species remained unclear because no authentic strains from Chodat were available for comparison. In particular, the status of *C. lacustris*, *C. rugosa*, and *C. cladoniae* cannot be resolved at present because of incomplete descriptions. The description of *C. lichina* is very similar to *Chloroidium ellipsoideum* or *C. angustoellipsoideum*. The major differences between *Chloroidium ellipsoideum* and *Chlorella lichina* is the presence of a granulated cell wall in the latter. Darienko *et al.* (2010) demonstrated that three out of four known *Chloroidium* species can produce granulated cell walls and that this feature is strain-specific, but not species-specific. Another feature that makes *Chlorella lichina* similar to *Chloroidium angustoellipsoideum* is the presence of peculiar globules (probably protein or satellite pyrenoids). The presence of these globules has also been observed in strain CCAP 211/108 and is strain-specific. Thus, *Chloroidium angustoellipsoideum* is a younger synonym of *Chlorella lichina*.

Chlorella viscosa is characterized by very similar morphology to that described for species of *Parachloroidium,* and strain SAG 56.87 and MG-3 (Fig. 6H–M). Unfortunately, Neustupa *et al.* (2013b) neglected morphological comparisons with previously described species such as those of Chodat in their description of the genus *Parachloroidium* and its species. The genus *Parachloroidium* was exclusively established on the basis of molecular phylogeny. Chodat (1913) described some difficulties in observing the pyrenoid in *Chlorella viscosa*, which became more visible after staining with Lugol solution. In descriptive cytology, Lugol solution was traditionally used to stain the starch envelope of pyrenoids. The naked pyrenoid (without starch) became visible as a white zone in the chloroplast after staining with Lugol solution. Neustupa *et al.* (2013b) demonstrated that *Parachloroidium* had a thylakoid-free zone in the chloroplast surrounded by small starch grains and associated with pyrenoglobuli. In this case, the same effect would be observed by staining with Lugol. The strains SAG 56.87 and MG-3 clearly demonstrated the presence of some structures that would be identified as naked pyrenoids in descriptive cytology after staining with Lugol solution. It is possible that this structure is also a thylakoid-free zone in the chloroplast. It seems to be a peculiarity of the *Watanabea* clade that this phenomenon was observed for the first time by Hanagata *et al.* (1998) in *Watanabea reniformis*.

As a results of our findings, we propose the following taxonomic changes including the description of new species and new combinations:

Chloroidium Nadson emend. Darienko & Pröschold
Synonym: *Chlorothecium* Krüger 1894 *non Chlorothecium* Borzi 1885, *Kruegera* Heering 1906, *Parachloroidium* Neustupa & Škaloud 2013

Emended diagnosis: Cells narrowly or broadly ellipsoidal, ellipsoidal to ovoid, or spherical; chloroplast parietal lobed or unlobed (but not cup-shaped), with or without pyrenoid, with or without starch grains surrounding pyrenoid; cell wall relatively thin, becoming thicker with age, sometimes forming a granular structure; and reproduction by unequal size autospores in small and large autosporangia, release of autospores by rupture of sporangial cell wall.
Type species: *Chloroidium saccharophilum* (Krüger) Darienko *et al.* (2010)

Chloroidium laureanum (Neustupa & Škaloud) Darienko & Pröschold comb. nov.
Basionym: *Parachloroidium laureanum* Neustupa & Škaloud in Neustupa *et al.* 2013, *Phycologia* 52: 413 (authentic strain: CAUP H8501, cryopreserved).

Chloroidium lobatum (Neustupa & Škaloud) Darienko & Pröschold comb. nov.
Basionym: *Parachloroidium lobatum* Neustupa & Škaloud in Neustupa *et al.* 2013, *Phycologia* 52: 413 (authentic strain: CAUP H8502, cryopreserved).

Chloroidium lichenum (Chodat) Darienko & Pröschold comb. nov.
Basionym: *Chlorella lichina* Chodat 1913, *Monogr. Alg. Cult. Pure*: 92, Fig. 16 (lectotype designated here).

Synonym: *Chloroidium angustoellipsoideum* (Hanagata & Chihara) Darienko *et al.* 2010, *Eur. J. Phycol.* 45: 93, *Chlorella angustoellipsoidea* Hanagata & Chihara in Hanagata *et al.* 1997, *Jap. J. Bot.* 72: 39.

Chloroidium antarcticum Darienko, Lukešová & Pröschold sp. nov.
Diagnosis: Young cells are ellipsoidal, broadly ellipsoidal to almost spherical, 13.6 × 10.9 µm–16.4 × 11.8 µm. Cell wall is relatively thin. Chloroplast is parietal, band-shaped, and deeply lobed. Mature vegetative cells ellipsoidal to broadly ellipsoidal 19.1 × 16.4–24.5 × 20.0 µm. Chloroplast is parietal, deeply lobed, and massive, with one naked pyrenoid. Nucleus is single, large, and is good visible. The cell wall of mature vegetative cells becomes slightly ticker. Cells accumulate some small vacuoles with age, which are located in the center or periphery of the cells and which sometimes slightly remove chloroplasts from the cell wall.

Reproduction determined by equal and unequal size of autospores. Autospores of equal size are produced at 8–64 per sporangium and have a narrowly ellipsoidal shape. Autosporangia of this type are 21.8 × 20.0 to 26.8 × 20.9 µm in size. Autospores in sporangia approximately 10.0 × 4.5 µm in size.

Autospores of unequal size were produced at a rate of 4–16 per sporangium. According to the cell shape and the size of autospores, they can by classified into three types. (i) autosporangia containing 4–8 spores, which contain large and small autospores of the same broadly ellipsoidal cell-shape. Large autospores are 15.5 × 13.5 µm in size, while small autospores are approximately 7.0 µm in size. (ii) Sporangia with 4–16 daughter cells, containing one large broadly ellipsoidal cell and other small narrowly ellipsoidal cells. Large autospores are 13.6 × 10.9–15.5 × 13.5 µm, and small are approximately 9.1 × 5.0 µm. (iii) Sporangia with 4 spores containing two large and two small broadly

ellipsoidal spores. Large autospores are 10.9 × 8.2–13.6 × 10.9 µm in size, and small are approximately 6.4–5.0 µm in size.

The liberation of autospores is achieved by apical rupturing of sporangia. The remains of sporangial cell wall are usually bag-shaped. The liberation of autospores continues for a long time after rupturing. Often, one autospore remains in the sporangial cell wall and develops into a mature vegetative cell.

Differs from other *Chloroidium* species by its larger cell size, different types of autosporangia and CBCs in its ITS-2.

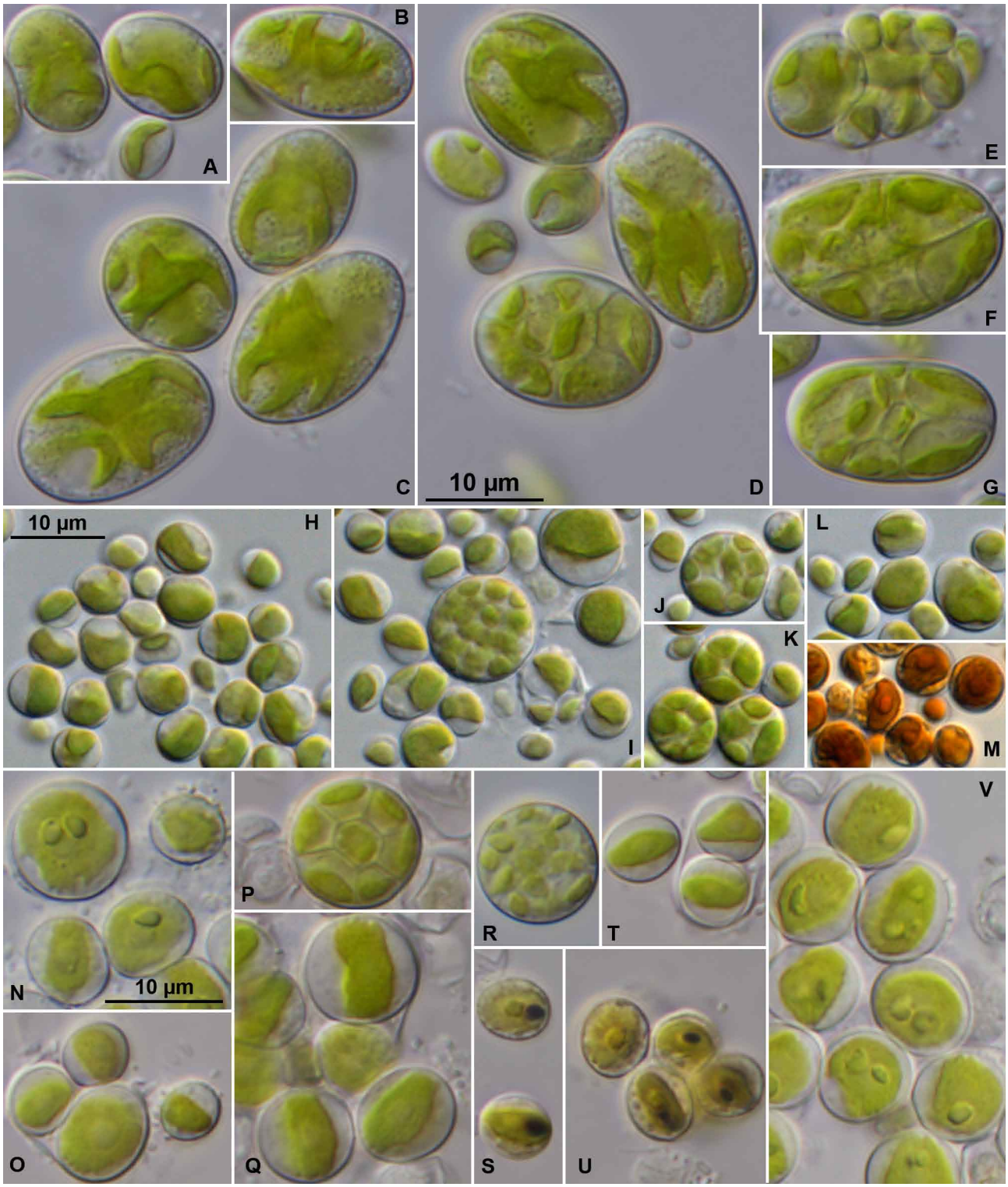

FIGURE 6. Morphology and phenotypic plasticity of the new *Chloroidium* species. **A.–G.** *C. antarcticum*; **H.–M.** *C. viscosum*; **N.–V.** *C. arboriculum*; scale bar = 10 µm.

Type locality: soil, South Shetlands, King George Island, Ecology Glacier, Antarctica.

Holotype (designated here): The strain ISBAL-1013 is cryopreserved in a metabolically inactive state at the SAG, Göttingen, Germany.

Iconotype (in support of the holotype designated here): Fig. 6A–G in this study.

Chloroidium viscosum (Chodat) Darienko & Pröschold comb. nov.

Basionym: *Chlorella viscosa* Chodat, 1913, Monographies d'algues en cultures pure, p. 105, Fig. 97 (lectotype designated here).

Emended Diagnosis: Young cells are ellipsoidal to broadly ellipsoidal, 4.1 × 2.8–5.6 × 5.0 µm. Cell wall is thin and smooth. Chloroplast is parietal and band-shaped with a smooth even margin, sometimes slightly removed from the cell wall. Pyrenoid is not distinct, naked, without a starch sheath, and becomes suffiently visible after staining with Lugol solution.

Mature vegetative cells ellipsoidal to almost spherical, 6.3 × 5.0–8.8 × 6.9 µm. Chloroplast is parietal, band-shaped, sometimes with a slightly wavy margin, and often removed from the cell wall. Cell wall of mature vegetative cells becomes slightly thicker in comparison with young cells. Nucleus is single, not distinct. Old cells are spherical, 9.4–10.0 µm in diameter. Chloroplast belt-like with a wavy margin, removed from the cell wall and similar to that of *Heterochlorella luteoviridis*.

Reproduction is done by autospores of equal and unequal size. Autosporangia with equally sized autospores usually contain 32 spores, while autosporangia with unequally sized contain 2–8 spores. Autosporangia are spherical, 7.5 to 12.0 µm in size. Large autospores have the same size as mature vegetative cells. Liberation of autospores happens via the rupturing of the sporangia. Often one autospore remains in the sporangial cell wall and develops into a mature vegetative cell.

Differs from the morphologically similar species *Heterochlorella luteoviridis* by the presence of a naked pyrenoid and absence of cytoplasm vacuolization. Differs from other species of *Chloroidium* by spherical cell shape and CBCs in its ITS-2.

Type locality: Photobiont of *Woessia fusarioides*, on trunk of *Quercus*, collected near Tatzmannsdorf, Burgenland, Austria (Tschermak-Woess, 1988).

Epitype (designated here): The strain SAG 56.87 is cryopreserved in a metabolically inactive state at the SAG, Göttingen, Germany.

Iconotype (in support of the holotype designated here): Fig. 6H–M in this study.

The second strain MG-2 was isolated in 2010 from free-living biofilm collected from the bark of tree of *Fagus sylvatica* in Vienna Forest. Note: The strain SAG 2338, designated as authentic strain of *Chlorella viscosa*, differed in its morphology and does not fit the original description provided by Chodat (1913). Our sequence (acc. no. MH551524) demonstrated that this strain is identical to *C. vulgaris*.

Chloroidium arboriculum Darienko & Pröschold sp. nov.

Diagnosis: Young cells are broadly ellipsoidal to spherical 4.1 × 2.8–5.6 × 5.0 µm. Cell wall is thin and smooth. Chloroplast is parietal and band-shaped with an even smooth margin, sometimes slightly removed from the cell wall. Pyrenoid is not distinct, naked, without a starch-sheath, and becomes highly visible after staining with Lugol solution.

Mature vegetative cells are ellipsoidal to almost spherical, 5.3 × 5.0–8.3 × 8.5 µm. Chloroplast is parietal, band-shaped, sometimes with a slightly wavy margin, and often removed from the cell wall. Cell walls of mature vegetative cells sometimes become granulated. Nucleus is single and not distinct. Old cells are spherical, 9.2–10.0 µm in diameter. Chloroplast is belt-like with a wavy margin, and is removed from the cell wall. Hollow spaces that could also be contrasted using the Lugol solution are also sometimes present in the cells.

Reproduction occurs by autospores of equal and unequal size. Autosporangia with equally sized autospores usually contain 4–8 spores. Autosporangia are spherical, 7.2 to 10.8 µm in size. Liberation of autospores occurs via the rupturing of sporangia.

Compared to morphologically similar *Parachloroidium laureanum*, *P. lobatum* differs by chloroplasts often being slightly removed from the cell wall and differences in its ITS-2 sequences. It is distinguished from *Chloroidium viscosum* only by changes in the ITS-2 sequences.

Type locality: Vienna Forest, bark of tree, free-living biofilm on *Fagus sylvatica*, near Vienna, Austria.

Holotype (designated here): The strain MG-3 is cryopreserved in a metabolically inactive state at the SAG, Göttingen, Germany.

Iconotype (in support of the lectotype designated here): Fig. 6N–V in this study.

Acknowledgement

We thank Katharina Freystein for isolating of five strains.

References

Aboal, M. & Werner, O. (2011) Morphology, fine structure, life cycle and phylogenetic analysis of *Phyllosiphon arisari*, a siphonous parasitic green alga. *European Journal of Phycology* 46: 181–192.
https://doi.org/10.1080/09670262.2011.590902

Akaike, H. (1974) A new look at the statistical model identification. *IEEE Transactions on Automatic Control* 19: 716–723.
https://doi.org/10.1109/TAC.1974.1100705

Albertano, P., Pollio, A. & Taddei, R. (1991) *Viridiella fridericiana* (Chlorococcales, Chlorophyta), a new genus and species isolated from extremely acid environments. *Phycologia* 30: 346–354.
https://doi.org/10.2216/i0031-8884-30-4-346.1

Altschul, S.F., Gish, W., Miller, W., Myers, E.W. & Lipman, D.J. (1990) Basic local alignment search tool. *Journal of Molecular Biology* 215: 403–410.
https://doi.org/10.1016/S0022-2836(05)80360-2

Andreyva, V.M. (1975) *Rod Chlorella. Morphologiya, sistematika, princypy klassifikatsii [The genus Chlorella. Morphology, systematics, principal classification]*. Nauka, Leningrad, 86 pp. [in Russian]

Chodat, R. (1913) Monographies d'Algues en culture pure. *Matériaux pour la Flore cryptogamique Suisse* 4: 1–266.

Clement, M., Posada, D. & Crandall, K.A. (2000) TCS: a computer program to estimate gene genealogies. *Molecular Ecology* 9: 1657–1659.
https://doi.org/10.1046/j.1365-294x.2000.01020.x

Clement, M., Snell, Q., Walker, P., Posada, D. & Crandall, K. (2002) TCS: Estimating gene genealogies. *Parallel and Distributed Processing Symposium, International Proceedings* 2: 184.
https://doi.org/10.1021/ja012036c

Coleman, A.W. (2000) The significance of a coincidence between evolutionary landmarks found in mating affinity and a DNA sequence. *Protist* 151: 1–9.
https://doi.org/10.1078/1434-4610-00002

Coleman, A.W. (2003) ITS2 is a double-edged tool for eukaryote evolutionary comparisons. *Trends in Genetics* 19: 370–375.
https://doi.org/10.1016/S0168-9525(03)00118-5

Cote, C.A., Greer, C.L. & Peculis, B.A. (2002) Dynamic conformational model for the role of ITS2 in pre-rRNA processing in yeast. *RNA* 8: 786–797.
https://doi.org/10.1017/S1355838202023063

Darienko, T., Gustavs, L., Mudimu, O., Rad Menendez, C., Schumann, R., Karsten, U., Friedl, T. & Pröschold, T. (2010) *Chloroidium*, a common terrestrial coccoid green alga previously assigned to *Chlorella* (Trebouxiophyceae, Chlorophyta). *European Journal of Phycology* 45: 79–95.
https://doi.org/10.1080/09670260903362820

Darienko, T., Gustavs, L., Eggert, A., Wolf, W. & Pröschold, T. (2015a) Evaluating the species boundaries of green microalgae (*Coccomyxa*, Trebouxiophyceae, Chlorophyta) using integrative taxonomy and DNA barcoding with further implications for the species identification in environmental samples. *PLOS One* 10: e0127838.
https://doi.org/10.1371/journal.pone.0127838

Darienko, T. & Pröschold, T. (2015b) Genetic variability and taxonomic revision of the genus *Auxenochlorella* (Shihira et Krauss) Kalina et Puncocharova (Trebouxiophyceae, Chlorophyta). *Journal of Phycology* 51: 394–400.
https://doi.org/10.1111/jpy.12279

Darienko, T., Gustavs, L. & Pröschold, T. (2016) Species concept and nomenclatural changes within the genera *Elliptochloris* and *Pseudochlorella* (Trebouxiophyceae) based on an integrative approach. *Journal of Phycology* 52: 1125–1145.
https://doi.org/10.1111/jpy.12481

Demchenko, E., Mikhailyuk, T., Coleman, A.W. & Pröschold, T. (2012) Generic and species concepts in *Microglena* (previously the *Chlamydomonas monadina* group) revised using an integrative approach. *European Journal of Phycology* 47: 264–290.
https://doi.org/10.1080/09670262.2012.678388

Do, C.B., Woods, D.A. & Batzoglou, S. (2006) CONTRAfold: RNA secondary structure prediction without physics-based models. *Bioinformatics* 22: e90–e98.
https://doi.org/10.1093/bioinformatics/btl246

Ettl, H. & Gärtner, G. (1995) *Syllabus der Boden-, Luft- und Flechtenalgen.* Stuttgart, Jena and Heidelberg: Gustav Fischer, 721 pp.

Ettl, H. & Gärtner, G. (2014) *Syllabus der Boden-, Luft- und Flechtenalgen.* Berlin and Heidelberg: Springer, 773 pp. https://doi.org/10.1007/978-3-642-39462-1

Fott, B. & Nováková, M. (1969) A monograph of the genus *Chlorella*. The fresh water species. *In*: Fott, B. (Ed.) *Studies in Phycology.* Academia, Prague, pp. 10–74.

Fučíková, K., Lewis, P.O. & Lewis, L.A. (2014) Widespread desert affiliation of trebouxiophycean algae (Trebouxiophyceae, Chlorophyta) including discovering of three new desert genera. *Phycological Research* 62: 294–305. https://doi.org/10.1111/pre.12062

Gibson, A., Gowri-Shankar, V., Higgs, P. & Rattray, M. (2005) A comprehensive analysis of mammalian mitochondrial genome base composition and improved phylogenetic methods. *Molecular Biology and Evolution* 22: 251–264. https://doi.org/10.1093/molbev/msi012

Hallmann, C., Hoppert, M., Mudimu, O. & Friedl, T. (2016) Biodiversity of green algae covering artificial hard substrate surfaces in a suburban environment: A case study using molecular approaches. *Journal of Phycology* 52: 732–744. https://doi.org/10.1111/jpy.12437

Hanagata, N., Karube, I. & Chihara, M. (1997) Bark-inhabiting green algae in Japan (3) *Chlorella trebouxioides* and *Ch. angusto-ellipsoidea*, sp. nov, (Chlorelloidea, Chlorellaceae, Chlorococcales). *Japanese Journal of Botany* 72: 36–43.

Hanagata, N., Karube, I., Chihara, M. & Silva, P.C. (1998) Reconsideration of the taxonomy of ellipsoid species of *Chlorella* (Trebouxiophyceae, Chlorophyta), with establishment of *Watanabea* gen. nov. *Phycological Research* 46: 221–229. https://doi.org/10.1111/j.1440-1835.1998.tb00117.x

Higgs, P., Jameson, D., Jow, H. & Rattray, M. (2003) The evolution of tRNA-Leu genes in animal mitochondrial genomes. *Journal of Molecular Evolution* 57: 435–445. https://doi.org/10.1007/s00239-003-2494-6

Hudelot, C., Gowri-Shankar, V., Jow, H., Rattray, M. & Higgs, P. (2003) RNA-based phylogenetic methods: application to mammalian mitochondrial RNA sequences. *Molecular Phylogenetics and Evolution* 28: 241–252. https://doi.org/10.1016/S1055-7903(03)00061-7

Huss, V.A.R., Frank, C., Hartmann, E.C., Hirmer, M., Klobouček, A., Seidel, B.M., Wenzeler, P. & Kessler, E. (1999) Biochemical taxonomy and molecular phylogeny of the genus *Chlorella sensu lato* (Chlorophyta). *Journal of Phycology* 35: 587–598. https://doi.org/10.1046/j.1529-8817.1999.3530587.x

Jow, H., Hudelot, C., Rattray, M. & Higgs, P. (2002) Bayesian phylogenetics using an RNA substitution model applied to early mammalian evolution. *Molecular Biology and Evolution* 19: 1591–1601. https://doi.org/10.1093/oxfordjournals.molbev.a004221

Krienitz, L. & Bock, C. (2012) Present state of the systematics of planktonic coccoid green algae of inland waters. *Hydrobiologia* 698: 295–326. https://doi.org/10.1007/s10750-012-1079-z

Leigh, J.W. & Bryant, D. (2015) POPART: Full-feature software for haplotype network construction. *Methods in Ecology and Evolution* 6: 1110–1116. https://doi.org/10.1111/2041-210X.12410

Ma, S., Huss, V.A.R, Tan, D., Sun, X., Chen, J., Xie, Y. & Zhang, J. (2013) A novel species in the genu *Heveochlorella* (Trebouxiophyceae, Chlorophyta) witnesses the evolution from an epiphytic into an endophytic lifestyle in tree-dwelling green algae. *European Journal of Phycology* 48: 200–209. https://doi.org/10.1080/09670262.2013.790996

Marin, B., Palm, A., Klingberg, M. & Melkonian, M. (2003) Phylogeny and taxonomic revision of plastid-containing euglenophytes based on SSU rDNA sequence comparisons and synapomorphic signatures in the SSU rRNA secondary structure. *Protist* 154: 99–145. https://doi.org/10.1078/143446103764928521

Neustupa, J., Němcová, Y., Eliás, M. & Škaloud, P. (2009) *Kalinella bambusicola* gen. et sp. nov. (Trebouxiophyceae, Chlorophyta), a novel coccoid *Chlorella*-like subaerial alga from Southeast Asia. *Phycological Research* 57: 159–169. https://doi.org/10.1111/j.1440-1835.2009.00534.x

Neustupa, J., Němcová, Y., Veselá, J., Steinová, J. & Škaloud, P. (2013a) *Leptochlorella corticola* gen. et sp. nov. and *Kalinella apyrenoidosa* sp. nov.: two novel *Chlorella*-like green microalgae (Trebouxiophyceae, Chlorophyta) from subaerial habitats. *International Journal of Systematic and Evolutionary Microbiology* 63: 377–387. https://doi.org/10.1099/ijs.0.047944-0

Neustupa, J., Němcová, Y., Veselá, J., Steinová, J. & Škaloud, P. (2013b) *Parachloroidium* gen. nov. (Trebouxiophyceae, Chlorophyta), a novel genus of coccoid green algae from subaerial corticolous biofilms. *Phycologia* 52: 411–421. https://doi.org/10.2216/13-142.2

Nozaki, H., Ito, M., Sano, R., Uchida, H., Watanabe, M.M. & Kuroiwa, T. (1995) Phylogenetic relationship within the colonial Volvocales (Chlorophyta) inferred from *rbc*L gene sequence data. *Journal of Phycology* 31: 970–979. https://doi.org/10.1111/j.0022-3646.1995.00970.x

Posada, D. (2008) ModelTest: phylogenetic model averaging. *Molecular Biology and Evolution* 25: 1253–1256. https://doi.org/10.1093/molbev/msn083

Procházková, K., Némcová, Y., Kulichová, J. & Neustupa, J. (2015) Morphology and phylogeny of parasitic and free-living members of the genus *Phyllosiphon* (Trebouxiophyceae, Chlorophyta). *Nova Hedwigia* 101: 501–518. https://doi.org/10.1127/nova_hedwigia/2015/0288

Procházková, K., Némcová, Y. & Neustupa, J. (2016) *Phyllosiphon ari* sp. nov. (*Watanabea* clade, Trebouxiophyceae), a new parasitic species isolated from leaves of *Arum italicum* (Araceae). *Phytotaxa* 283: 143–154. https://doi.org/10.11646/phytotaxa.283.2.3

Procházková, K., Némcová, Y. & Neustupa, J. (2018) *Phyllosiphon duini* sp. nov. (Trebouxiophyceae, Chlorophyta), a species isolated from a corticolous phototrophic biofilm. *Cryptogamie, Algologie* 39: 23–34. https://doi.org/10.7872/crya/v39.iss1.2018.23

Pröschold, T., Darienko, T., Krienitz, L. & Coleman, A.W. (2018) *Chlamydomonas schloesseri* sp. nov. (Chlamydophyceae, Chlorophyta) revealed by morphology, autolysin cross experiments, and multiple gene analyses. *Phytotaxa* 362: 21–38. https://doi.org/10.11646/phytotaxa.362.1.2

Ronquist, F., Teslenko, M., Van Der Mark, P., Ayres, D.L., Darling, A., Höhna, S., Larget, B., Liu, L., Suchard, M.A. & Huelsenbeck, J.P. (2012) MrBayes 3.2: Efficient Bayesian phylogenetic inference and model choice across a large model space. *Systematic Biology* 61: 539–542. https://doi.org/10.1093/sysbio/sys029

Schlösser, U.G. (1997) Additions to the culture collections of algae since 1994. *Botanica Acta* 110: 424–429. https://doi.org/10.1111/j.1438-8677.1997.tb00659.x

Song, H., Zhang, Q., Liu, G. & Hu, Z. (2015) *Polulichloris henanensis* gen. et sp. nov. (Trebouxiophyceae, Chlorophyta), a novel subaerial coccoid green alga. *Phytotaxa* 218: 137–146. https://doi.org/10.11646/phytotaxa.218.2.3

Song, H., Hu, Y., Zhu, H., Wang, Q., Liu, G. & Hu, Z. (2016) Three novel species of coccoid green algae within the *Watanabea* clade (Trebouxiophyceae, Chlorophyta). *International Journal of Systematic and Evolutionary Microbiology* 66: 5465–5477. https://doi.org/10.1099/ijsem.0.001542

Stamatakis, A. (2006) RAxML-VI-HPC: maximum likelihood-based phylogenetic analyses with thousands of taxa and mixed models. *Bioinformatics* 22: 2688–2690. https://doi.org/10.1093/bioinformatics/btl446

Swofford, D.L. (2002) *PAUP* Phylogenetic Analysis Using Parsimony (*and Other Methods). Version 4.0b10.* Sunderland, MA, USA: Sinauer Associates.

Telford, M.J., Wise, M.J. & Gowri-Shankar, V. (2005) Consideration of RNA secondary structure significantly improves likelihood-based estimates of phylogeny: examples from the bilateria. *Molecular Biology and Evolution* 22: 1129–1136. https://doi.org/10.1093/molbev/msi099

Tschermak-Woess, E. (1988) New and known taxa of Chlorella (Chlorophyceae): occurrence as lichen photobionts and observations on living dictyosomes. *Plant Systematics and Evolution* 159: 123–139. https://doi.org/10.1007/BF00937430

Xia, X. (2018) DAMBE7: New and improved tools for data analysis in molecular biology and evolution. *Molecular Biology and Evolution* 35: 1550–1552. https://doi.org/10.1093/molbev/msy073

Xia, X., Xie, Z., Salemi, M., Chen, L. &Wang, Y. (2003) An index of substitution saturation and its application. *Molecular Phylogenetics and Evolution* 26: 1–7. https://doi.org/10.1016/S1055-7903(02)00326-3

Xia, X. & Lemey, P. (2009) Assessing substitution saturation with DAMBE. *In*: Lemey, P., Salemi, M. & Vandamme, A.-M. (Eds.) *The Phylogenetic Handbook: A Practical Approach to DNA and Protein Phylogeny. 2nd edition.* Cambridge University Press, pp. 615–630. https://doi.org/10.1017/CBO9780511819049.022

Yang, Z., Nielsen, R. & Hasegawa, M. (1998) Models of amino acid substitution and applications to mitochondrial protein evolution. *Molecular Biology and Evolution* 15: 1600–1611. https://doi.org/10.1093/oxfordjournals.molbev.a025888

Zhang, J., Huss, V.A.R., Sun, X., Chang, K. & Pang, D. (2008) Morphology and phylogenetic position of a trebouxiophycean green alga (Chlorophyta) growing on the rubber tree, *Hevea brasiliensis*, with the description of a genus and species. *European Journal of Phycology* 43: 185–193. https://doi.org/10.1080/09670260701718462

Zuker, M. (2003) Mfold web server for nucleic acid folding and hybridization prediction. *Nucleic Acid Research* 31: 3406–3615. https://doi.org/10.1093/nar/gkg595

Supplemental material:

Table S1. Strains used in this study.

Table S2. Haplotype designations of the gene regions (SSU, ITS-1 and ITS-2) and ITS-2 barcodes as well as the grouping to geographical region and habitats (used for the TCS networks; see Figs. 4-5) for each *Chloroidium* strain. The accession numbers of SSU and ITS rDNA sequences and the intron positions if present are also given in this table.

Figures S1. Additional analyses to the molecular phylogeny of representatives belonging to the *Watanabea* clade based on *rbc*L sequence comparisons. The saturation rates of each codon base were calculated using the tests introduced by Xia *et al.* (2003) and Xia & Lemey (2009) implemented in DAMBE (Xia, 2018) and summarized in the table. The phylogenetic tree using the dataset of all three codon bases (1206 bp) and the codon model YNH98 (Yang *et al.* 1998) were calculated in PHASE. The other trees shown were inferred based on different data sets (**A.** 402 amino acids, **B.** 804 and **C.** 1206 aligned positions of 58 taxa) using PAUP 4.0b10. The analyses shown in **A.** and **B.-C.** represented the results using neighbor-joining method and maximum likelihood, respectively.

Figures S2. ITS-2 secondary structures of the *Chloroidium* strains investigated in this study. The barcode region is numbered in white boxes and marked in blue for each helix. The line structure of the ITS-2 has been drawn with PseudoViewer (http://pseudoviewer.inha.ac.kr).